Electrochemically Controlled Hydrogels with Electrotunable Permeability and Uniaxial Actuation

Tobias Benselfelt,* Jyoti Shakya, Philipp Rothemund, Stefan B. Lindström, Andrew Piper, Thomas E. Winkler, Alireza Hajian, Lars Wågberg, Christoph Keplinger, and Mahiar Max Hamedi*

The unique properties of hydrogels enable the design of life-like soft intelligent systems. However, stimuli-responsive hydrogels still suffer from limited actuation control. Direct electronic control of electronically conductive hydrogels can solve this challenge and allow direct integration with modern electronic systems. An electrochemically controlled nanowire composite hydrogel with high in-plane conductivity that stimulates a uniaxial electrochemical osmotic expansion is demonstrated. This materials system allows precisely controlled shape-morphing at only −1 V, where capacitive charging of the hydrogel bulk leads to a large uniaxial expansion of up to 300%, caused by the ingress of ≈700 water molecules per electron–ion pair. The material retains its state when turned off, which is ideal for electrotunable membranes as the inherent coupling between the expansion and mesoporosity enables electronic control of permeability for adaptive separation, fractionation, and distribution. Used as electrochemical osmotic hydrogel actuators, they achieve an electroactive pressure of up to 0.7 MPa (1.4 MPa vs dry) and a work density of ≈150 kJ m^{-3} (2 MJ m^{-3} vs dry). This new materials system paves the way to integrate actuation, sensing, and controlled permeation into advanced soft intelligent systems.

1. Introduction

Hydrogels are among the best options for designing life-like soft intelligent systems[1] due to their tissue-like softness and high water content that allows the mass-transport of large amounts of ions and molecules to regulate shape, function, and ionotronic computation.[2–6] New multifunctional hydrogels can thus enable future machines with dynamic capabilities beyond current technologies.[5,7,8] Furthermore, multifunctionality can be easily integrated into hydrogel heterostructures,[9] like in living organisms, for example, using 3D printing.

Ideal stimuli-responsive hydrogels embed multifunctionality electronically in their bulk structure to seamlessly integrate with modern batteries and computers. However, current state-of-the-art stimuli-responsive hydrogels are not electronically conductive and require activation by external stimulation from changes in temperature,[10] pH,[11] and light[7,12] or rigid external electrodes,[13] limiting their performance in advanced heterostructures. We have previously shown that the fastest hydrogel actuators can be achieved by anisotropic fibrillar hydrogels, where the uniaxial expansion leads to fast and high strain.[14] Like these examples, most hydrogel actuators only activate or speed up a passive, diffusion-limited swelling mechanism using, often irreversible, stimulations.

T. Benselfelt, J. Shakya, A. Piper, A. Hajian, L. Wågberg, M. M. Hamedi
Department of Fibre and Polymer Technology
School of Engineering Sciences in Chemistry
Biotechnology and Health
KTH Royal Institute of Technology
Stockholm 100 44, Sweden
E-mail: bense@kth.se; mahiar@kth.se

P. Rothemund, C. Keplinger
Robotic Materials Department
Max Planck Institute for Intelligent Systems
70569 Stuttgart, Germany

S. B. Lindström
Department of Management and Engineering
Division of Solid Mechanics
Linköping University
Linköping 58183, Sweden

T. E. Winkler
Institute of Microtechnology & Center of Pharmaceutical Engineering
Technische Universität Braunschweig
38106 Braunschweig, Germany

C. Keplinger
Paul M. Rady Department of Mechanical Engineering
University of Colorado
Boulder, CO 80309, USA

C. Keplinger
Materials Science and Engineering Program
University of Colorado
Boulder, CO 80309, USA

Electronic control of hydrogel fibers was previously achieved by pH changes due to electrolysis around an embedded metal electrode at high voltage.[15,16] However, the lack of dynamic and precise shape control of truly soft hydrogel materials at low voltage is still a pressing challenge.

Here, we report an anisotropic nanowire composite hydrogel with high electron conductivity, adding electronic control to anisotropic fibrillar hydrogel actuators.[14] Electronic stimulation of the hydrogel increases the electrochemical osmotic (ECO) swelling pressure, enabling direct and dynamic electronic control of its uniaxial shape-morphing. The control is achieved by electrochemical charging to overcome and reverse the internal backbone charge, allowing precise control of the local microenvironment inside the hydrogel.

Electronically tunable (electrotunable) shape-morphing enables uniquely precise control of the porosity of the ECO hydrogel, increasing it by up to 400%. Its state is retained after the electrical potential is turned off because of the stick-slip-stick behavior of nanowire networks.[17,18] The shape-morphing can thus be controlled with high precision, and the degree of expansion can be self-sensed by measuring the varying electronic resistance.[7] These properties make nanowire hydrogels an ideal material for electrotunable membranes for adaptive separation, fractionation, and distribution of, for example, drugs or biomolecules; a unique and innovative membrane technology.

The in-plane stiffness of the ECO hydrogel transduces the swelling pressure into expansion in the out-of-plane direction without needing crosslinking or encapsulation, which limits the expansion and expansion rate for polymer hydrogels[10] or turgor actuators.[13] This new hydrogel material is thus also a substantial advance for hydrogel actuators as its robust nanowire network enables electronic controllability with high actuation stresses (0.7 MPa vs the passively swollen state or 1.4 MPa vs the dry state) and, at the same time, high uniaxial expansion (300% vs the passively swollen state or 1100% vs the dry state) with a high actuation rate (130% min^{-1} vs the passively swollen state or >600% min^{-1} vs the dry state). The maximum controllable expansion far exceeds that of most actuators, including turgor actuators (<50%)[13] and conducting polymer actuators (<40%).[19] These ECO hydrogel actuators can generate a volumetric force of ≈10 000 N cm^{-3}, two orders of magnitude larger than previous work.[13] The electronically controlled expansion beyond the passive baseline swelling is ≈10 times larger than previous reports for electroactive hydrogels, with at least three times higher actuation rate.[13] A significant advantage over electroosmotic hydrogel actuators[13,20] is the possibility for direct electronic control of the hydrogel without external electrodes at high voltages that may interfere with applicability, paving the way for integrating actuation, sensing, and controlled permeation into multifunctional soft intelligent systems.

2. Results and Discussion

The ECO hydrogels are fabricated from inexpensive and widely available cellulose nanofibrils (CNFs) and carbon nanotubes (CNTs), using a simple vacuum filtration process easily replicated with standard laboratory equipment (**Figure 1a**). CNFs are high aspect ratio nanoparticles of crystalline cellulose (Figure S1a, Supporting Information): the structural building block of trees and plants. They are extracted by chemical modification and mechanical disintegration of wood pulp and, as such, are ubiquitously available, renewable nanomaterials used to fabricate nanostructured materials.[21] CNFs are highly efficient dispersing agents for CNTs (Figure S1b, Supporting Information) in water, resulting in the formation of colloidal CNF/CNT complexes stabilized by the charge of the CNFs (Figure 1a).[22] These complexes permit a simple route to fabricate strong and homogeneous CNT composites on a large scale from aqueous dispersions for various advanced applications.[23,24] These nanowire composites have been used in several dry applications but never as electroactive hydrogels containing mostly water. Here, CNFs allow the manufacturing of hydrogels by providing a hydrophilic matrix that prevents irreversible cohesion of the conducting CNTs, while maintaining open yet strong fibrillar hydrogel networks that are difficult to achieve with polymers.[25,26]

During the filtration process, the CNF/CNT complexes self-assemble into stratified layers in the plane of the sheets (Figure 1b,c) with pore sizes on the order of 20 nm. By immersing the dry sheets in water, their anisotropy leads to uniaxial swelling to form ECO hydrogels (Figure 1d).[25] The densely packed, ordered layers allow high in-plane electronic conductivity, while the more randomly packed porous networks in-between permit fast transport of ions and water during the uniaxial swelling. The balance between the chemical charge of the CNFs and the electrochemical charge of the CNTs determines the osmotic pressure inside the hydrogel, enabling controlled uniaxial ECO expansion (Figure 1e).

ECO hydrogels are fundamentally different from polymer hydrogels since their behavior cannot be described by classical polymer physics. Instead of being entropy elastic, like polymer networks, they deform plastically via a stick-slip-stick behavior and, as a result, show emergent properties atypical of soft materials. For example, the ECO expansion can be paused and locked by electrochemical control (retained state), thanks to the stick-slip-stick deformation[17]—a feature not possible using polymer hydrogels.

The coupling between the expansion and structure of the network leads to two additional features: i) The increased electric resistance of the nanowire network upon expansion allows self-sensing and possible feedback control of the actuation (Figure 1e). ii) The inherent relation between expansion, pore size, resistance, and the retained state is ideal for developing electrotunable membranes with adaptive mesoporosity relevant for the permeation of larger molecules (Figure 1f).

To stimulate the ECO hydrogel, we connect it directly to an electric cable and apply a low voltage of ±1 V to capacitively charge/discharge the CNTs in the bulk of the hydrogel (Figure 1e). We note that the main electrochemical reaction here is non-faradaic, but these systems also work with pseudocapacitive charging as we have shown with MXene in a parallel work[27] and may also work with faradaic processes. Inserted electrons are compensated by Na$^+$ from the solution, resulting in a flux of ions into the bulk of the hydrogel, transducing the ECO pressure into uniaxial expansion. We propose that the average charge in the bulk of the hydrogel, which is the sum of the electrochemical charges of the CNTs and chemical charges of the CNFs, controls the swelling in three regimes for anionic CNFs (the opposite applies for cationic CNFs):
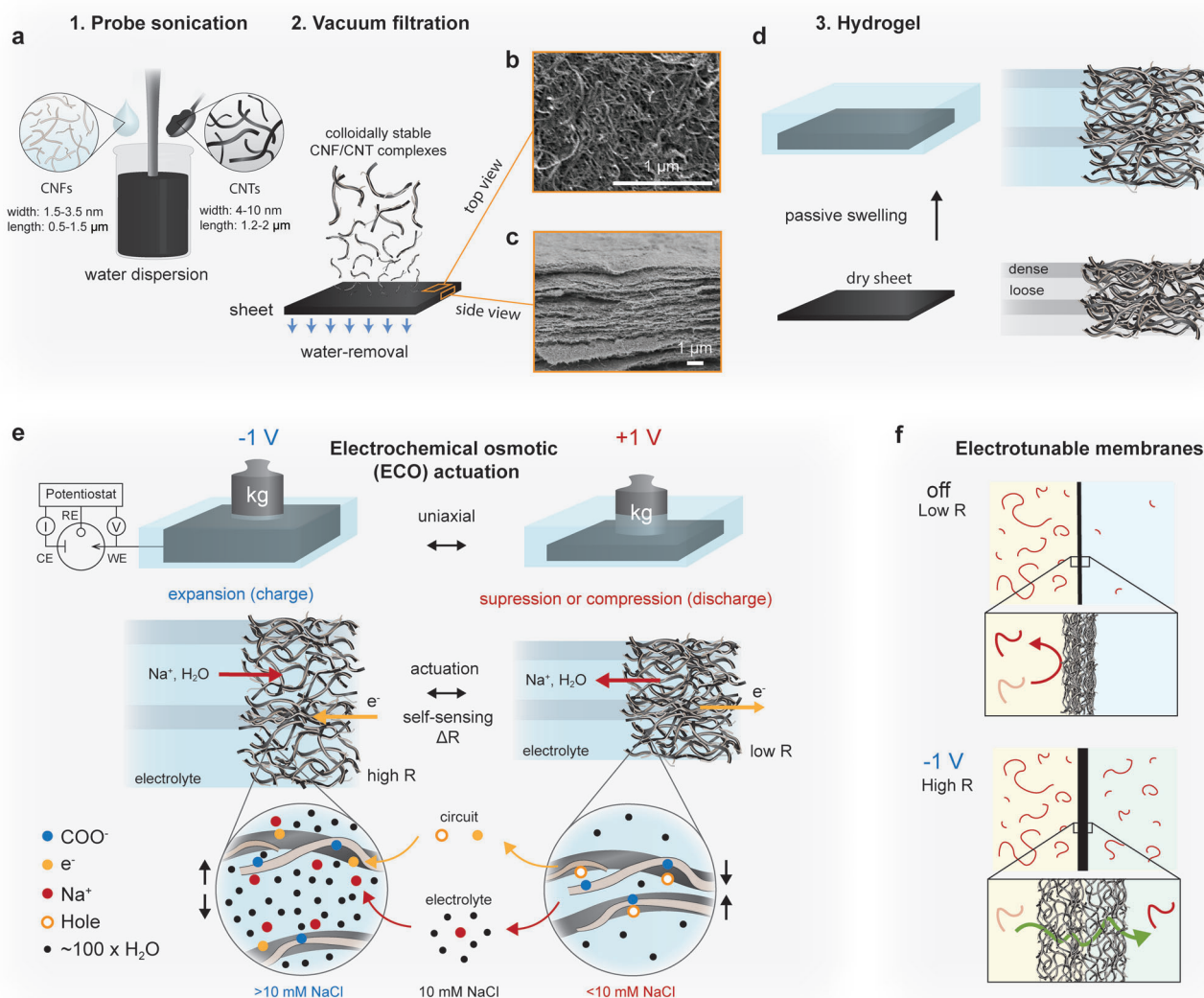
**ADVANCED
SCIENCE NEWS**

www.advancedsciencenews.com

**ADVANCED
MATERIALS**

www.advmat.de

Figure 1. Electrochemical osmotic actuators from ECO hydrogels. a) Schematic illustration of the formation of CNF/CNT complexes and their assembly into a sheet using vacuum filtration. b) Top-view, and c) cross-sectional SEM electrographs of a composite containing 60% CNTs. d) Schematic of the structure and swelling of the hydrogel. e) Schematic overview and detailed mechanistic description of the electrochemical osmotic actuation, including the self-sensing capability. The shaded areas are used to highlight looser and denser regions. f) Schematic of how the coupling between expansion and pore size enables electronically tunable membranes on the mesoporous scale.

i. The negative potential regime: Here, the capacitive double-layer charge of CNTs adds to the negative chemical charge of the CNFs, resulting in an increased swelling pressure.

ii. The potential of zero charge (PZC) regime: Here, a slight positive capacitive charge of the CNTs matches the negative chemical charge of CNFs, resulting in a net-zero charge and the absence of ion-driven swelling.

iii. The positive potential regime: Here, the positive capacitive charge of CNTs surpasses the negative chemical charge of CNFs, and the network is held together by ionic interactions that prevent swelling.

We used a three-electrode setup to test this hypothesis and investigate these regimes (Figure S2, Supporting Information; Ag/AgCl reference electrode). The influence of the applied po-

tential in these regimes is shown in **Figure 2**a and displays two features: for ECO hydrogels with 55% CNFs in 10 mM NaCl, voltages between 0 to −3 V show an additional ECO expansion of >100% compared to the passive swelling, whereas 0 to +3 V shows a 25% reduction in swelling. At a lower salt concentration of 0.1 mM or a lower CNT content of 30%, the ECO expansion was greater, reaching up to 300% (Figures S3a and S4, Supporting Information), by far exceeding the values of a few percent for double layer actuation of CNT sheets and approaching the electrochemical pneumatic expansion of the same sheets.[28] In the case of 40% cationic CNFs in 10 mM NaCl, these regimes changed order, supporting the hypothesis of the charge balance regimes. Although we used higher potentials, the operating range is ideally kept within a low voltage boundary (≈±1 V) to avoid unwanted electrochemical reactions with the saline solution. It is an

**ADVANCED
SCIENCE NEWS**

www.advancedsciencenews.com
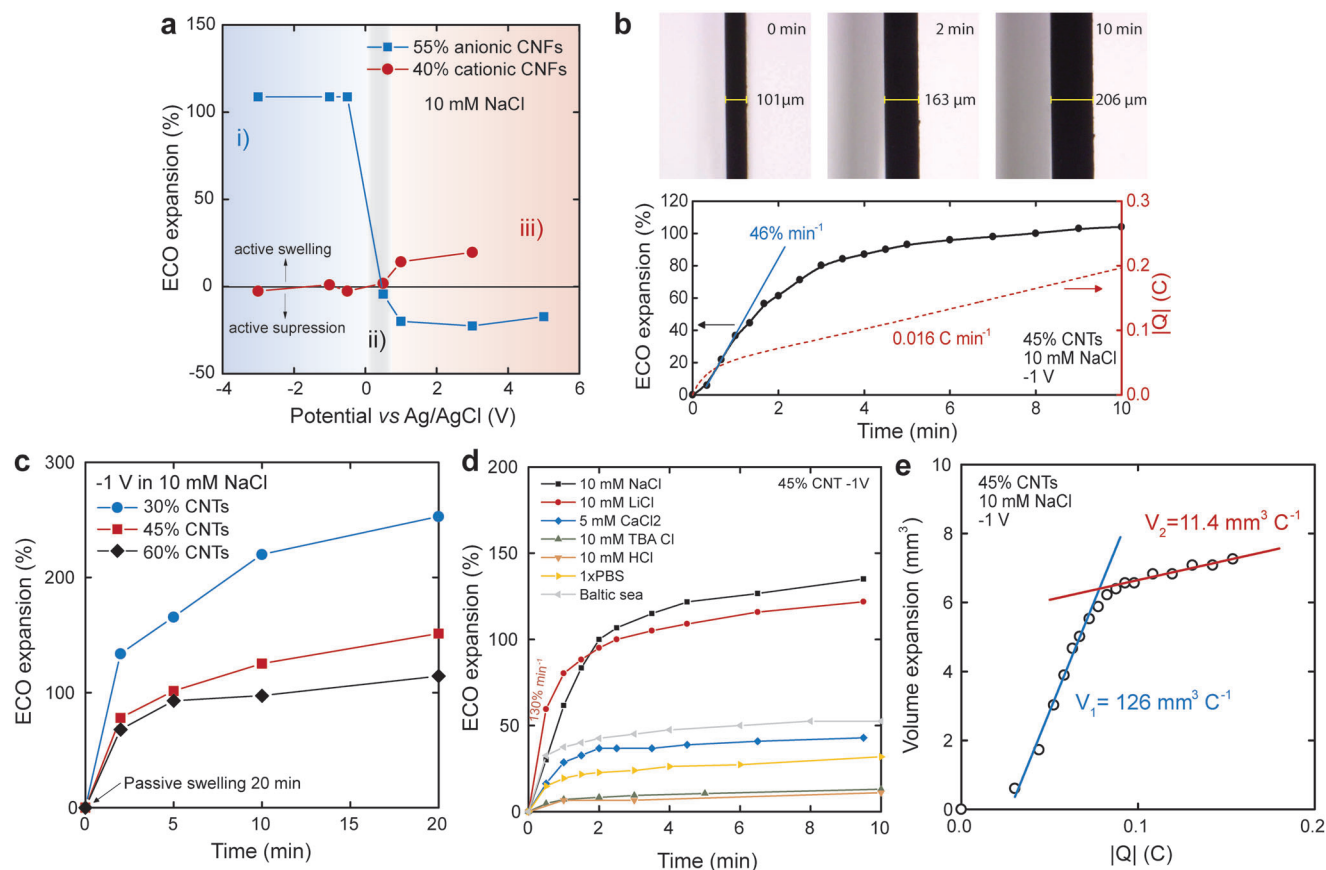
**ADVANCED
MATERIALS**

www.advmat.de

Figure 2. Electrochemical swelling regimes of ECO hydrogels. a) ECO expansion of hydrogels as a function of applied potential in 10 mM NaCl. b) Snapshot from the recorded ECO expansion of a hydrogel at −1 V, including the charge accumulation as a function of time. c) ECO expansion as a function of time for different CNT contents. d) ECO expansion of an ECO hydrogel as a function time at an applied voltage of −1 V in different electrolyte solutions. e) Volume expansion as a function of the capacitive charge increase in the sheet during swelling.

advantage that most of the expansion occurs within this voltage window.

To characterize the actuation at low voltages, we captured real-time microscopy images of an expanding ECO hydrogel comprising 55% anionic CNFs in 10 mM NaCl (Figure 2b). The initial expansion rate was 46% min^{-1}, and the hydrogel expanded by 60% in 2 min and 100% in 10 min from its equilibrium at the passively swollen state. During the first 30 s, the capacitive charge builds up rapidly (Figure 2b) and reaches a constant rate of 0.016 C min^{-1}, limited by the penetration of ions and water into the gradually expanding network. Although the capacitive charge increases, the degree of swelling approaches equilibrium due to the restricting nanowire network. A higher content of hydrophobic CNTs increases this restriction by a higher cohesion in water and, thus, lower expansion, as shown in Figure 2c.

We measured the ECO expansion in other electrolytes (Figure 2d). LiCl (10 mM) increased the actuation rate to 130% min^{-1}, whereas CaCl$_2$ and PBS led to a lower expansion due to the known interactions between CNFs and Ca^{2+} and the higher salinity of PBS. The influence of different ions on the swelling of CNF sheets has been studied elsewhere.[29,30]

In 10 mM HCl, almost no expansion was observed due to the protonation of carboxylic groups leading to stronger cohesion by van der Waals interactions according to fundamental colloidal sci-

ence. Bulky, more hydrophobic cations in tetrabutylammonium chloride also suppressed the swelling, indicating that the size of the ions or their hydration affects their penetration. Finally, the actuator expanded by 50% in seawater, demonstrating applications outside a clinical lab environment.

This data shows three essential features of stimuli-responsive ECO hydrogels: i) their speed can be increased using smaller ions; ii) they function in PBS and similar buffers making them applicable to biological in-vivo and in-vitro applications; iii) they work in seawater, making them applicable for marine applications, also under high pressure in deep water since hydrogels are incompressible. The low voltage makes them unproblematic in seawater or in contact with biological materials, for example, compared to dielectric elastomers, which must be encapsulated.[31]

The volumetric expansion as a function of capacitive charge displays two different rates (Figure 2e): a fast initial rate, V_1 = 126 mm^3 C^{-1}, and a slow rate, V_2 = 11.4 mm^3 C^{-1}, at steady-state swelling. We propose that V_1 corresponds to fast swelling in-between layers where most CNTs are charged, forming electrical double layers. The second regime, V_2, corresponds to further charging of the CNTs as more sites become available in the bulk of the hydrogel upon the slower swelling of the denser layers. We note, however, that the majority of swelling comes from

**ADVANCED
SCIENCE NEWS**

www.advancedsciencenews.com

**ADVANCED
MATERIALS**

www.advmat.de

the initial capacitive charging. We calculated the number of water molecules (based on volumetric expansion, mm^3) per electron–ion pair (based on capacitive charge, C) to be as high as 682 for V_1, which is 100 times more than for actuators from CNTs and polyanions.[32] This movement of unperturbed water is consistent with bulk osmotic pressure and not only the insertion of hydrated ions as for capacitive actuators.[32]

Further characterization shows that the expansion rate is smaller at lower potentials (Figure S3b, Supporting Information) since it takes longer to build up the required electrochemical charge to reach a critical ECO pressure. We observe similar behavior in an electrolyte of lower concentration (Figure S3c, Supporting Information) due to the local depletion of ions and a higher electrolyte resistance.

We used electrochemical impedance spectroscopy to characterize the PZC regime (Figure S5, Supporting Information). Figure S6 (Supporting Information) shows a PZC of $\approx$+0.3 V that increases with decreasing CNT content since a higher CNT potential is required to compensate for the potential of the chemical charge of the CNFs. The PZC was also influenced by the salt concentration, which affects the resistance and buffering capacity of the electrolyte as later shown by the Poisson–Boltzmann simulation (supporting information).

To better understand the electromechanical behavior of ECO hydrogels, we propose an analytic model obtained by expanding the Flory and Rehner polymer gel model to include nanoparticle networks. Our model describes the swelling pressure induced by the changed chemical potential when mixing the gel constituents with the solvent (P_{chem}) and the elastoplastic resistance during the expansion of the network (P_{net}). For polymer networks, an entropy elastic Gaussian chain model can be used,[10] but there is not yet a quantitative model for enthalpy elastic nanoparticle networks; these are qualitatively described by the initial bending of fibrils under pressure followed by a plastic stick-slip-stick behavior as previously described by Mittal et al. and Östmans et al.[17,18] In our electroactive nanoparticle gel model (see Supporting Information), P_{chem} is divided into the terms P_{mix}, the free energy of mixing contributing to passive swelling, and P_{ion}, the osmotic pressure from the chemical and electrochemical charge inside the hydrogel:

$$P_{ion} = RT \left(\frac{\varphi_1 \alpha Q_{CNF}}{V} + \frac{\varphi_2 Q_{CNT}}{V} - \varphi_3 2 c_{sol} \right) \tag{1}$$

where R is the gas constant, T is the absolute temperature, Q is the molar charge associated with the CNFs or CNTs including counterions, α is the degree of dissociation/association of the titrating groups of the CNFs, φ_n are the osmotic coefficients with the subscript describing different ion-pairs, V is the volume of the hydrogel, and c_{sol} the molar concentration of the electrolyte multiplied by 2 to account for both ions in the pair. Equation (1) shows how Q_{CNF}, Q_{CNT}, or c_{sol} control the osmotic pressure. Q_{CNT} is the only parameter that can be dynamically changed via electric stimulation, whereas the others can be tailored for the working conditions, as seen by data in Figure 2 and Figure S3 (Supporting Information). For example, increasing the charge density of the CNFs results in a more significant expansion (Figure S8, Supporting Information). P_{net} and P_{mix} are primarily governed by the CNT content (Figure S9, Supporting Information) since increasing CNT concentrations lead to more cohesion (Figure 2c; Figure S3a, Supporting Information).

To further test our model and show that an electrochemically induced osmotic pressure drives the expansion of ECO hydrogels, we measured the influence of salt concentration (c_{sol}), which is the basis for the osmotic pressure difference in Equation (1). The passive swelling is only slightly affected by the salt concentration since P_{mix} dominates (Figure S10a, Supporting Information) In contrast, the ECO expansion is reduced at salt concentrations above 10 mM due to the diminishing difference between internal and external salt concentrations.[25] At 100 mM NaCl the achieved expansion is much lower and this is the qualitative limit for highly expanding ECO actuators (Figure S10a, Supporting Information). Data derived from Equation (1) (Figure S10b, Supporting Information) shows that the idealized model for osmotic pressure can predict the influence of salt in Figure S10a (Supporting Information). Equation (1) can thus be used to determine suitable working conditions and predict behaviors.

The experiments and analytical model do not capture local mechanisms inside the hydrogel network, such as the degree of dissociation (α in Equation (1)). To further develop our theoretical model for this class of materials, we used a 2D Poisson–Boltzmann simulation (see details in Figure S11, Supporting Information). The simulation agrees with the experimental data and shows that α depends on the electrolyte concentration due to an increased buffering capacity at higher concentrations. A positive potential of the CNTs also increases α due to the local repulsion of hydronium ions, thus an electrochemically controlled degree of dissociation that also influences the swelling pressure.

To further investigate the dynamic control of the shape-morphing, we studied the expansion while switching on and off the potential during the swelling (**Figure 3**a). The expansion could be controlled in steps by activating (-0.5 V) and deactivating ($+0.5$ V) the ECO pressure. An exciting feature is that the network locks in the new state (retained state Figure 3a) when the potential is turned off or switched to positive since the stick-slip-stick behavior of nanowire networks dissipates the elastic energy by plastic relaxation. The pressure acting to de-swell the network is not high enough to overcome the fibril network, which is almost equally stiff in expansion and compression.

The direct electronic control without external rigid electrodes and the retained state are undoubtedly unique and valuable features of ECO hydrogels. Another feature is that expansion of the network decreases the percolation of the conducting CNT network and increases its in-plane electric resistance. The relative resistance of the hydrogel $(R - R_0)/R_0$ is directly proportional to the swelling in deionized water (Figure 3b; Figure S12, Supporting Information). However, the change is small due to the anisotropy of the network. We measured this in deionized water to have maximum swelling to measure the widest possible percolation range and to avoid the influence of ionic conductivity.

The CNTs throughout the hydrogel can thus be charged at low voltages even in a highly expanded state containing 70–90 vol% water. The relative in-plane resistance still enables an electrical self-sensing modality with a gauge factor of 1.4. The self-sensing by the electric resistance opens possibilities for advanced feedback control of the dynamically controlled ECO expansion.

The dynamic control, the retained state, and self-sensing allow stepwise control and locking it at defined values. The
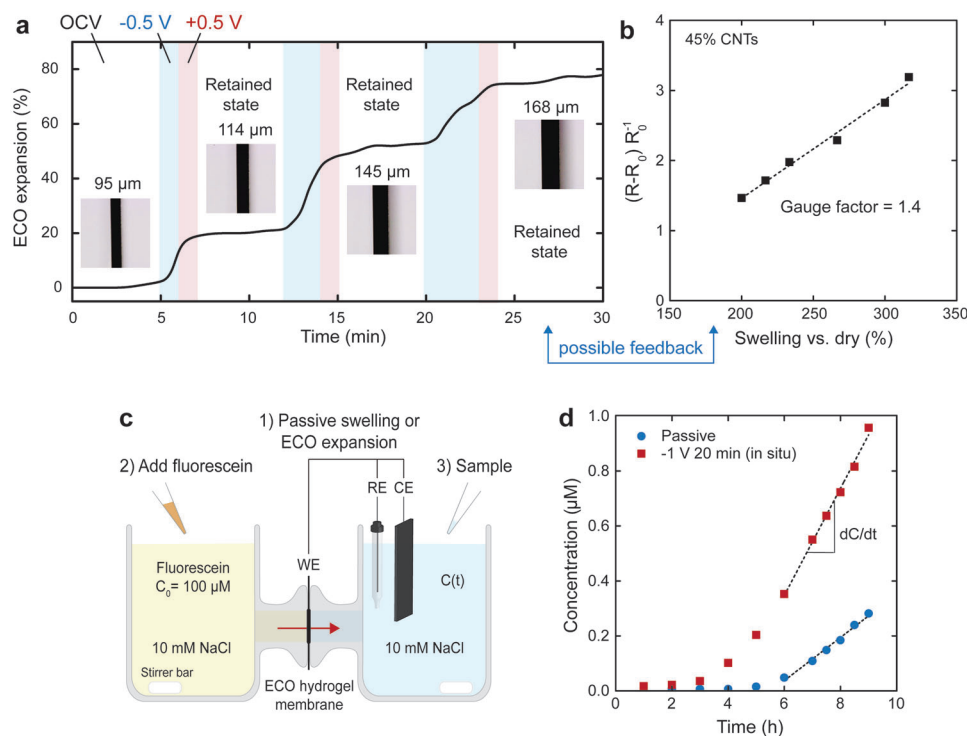
**ADVANCED
SCIENCE NEWS**

www.advancedsciencenews.com

**ADVANCED
MATERIALS**

www.advmat.de

Figure 3. Electronically tunable membranes from ECO hydrogels. a) Stepwise ECO expansion of a hydrogel, "OCV" is the open current voltage. b) Relative in-plane electric resistance of the hydrogel as a function of swelling. c) The setup used to measure membrane permeability. d) Concentration in the accepting chamber as a function of time. The conditions are 45% CNTs and 10 mM NaCl.

inherent relationship between the swelling and the porosity of the hydrogel network thus allows precise control of the pore size, enabling electronically tunable membranes. Figure 3c illustrates the permeability measurement setup used to demonstrate the electrotunable membrane concept, using fluorescein as a model compound. The increased concentration of fluorescein ($C(t)$) in the accepting chamber separated by a passively swollen hydrogel membrane or a membrane after 20 min of expansion at −1 V is shown in Figure 3d, corresponding to an increased apparent permeability index of 140% in the ECO-expanded state (Figure S13, Supporting Information).

Tunable membranes reported in the literature are few and mainly made from dense conducting polymers or graphene sheets that exhibit a 20–30% increase in small molecule permeation.[33,34] ECO hydrogels demonstrate applicability as membranes with electronically-controlled mesoporosity, making them suited for adaptive separation, fractionation, and distribution of a broader range of molecules. The ability to work in harsh environments, PBS (for in-vivo application), and seawater is promising for future developments.

We characterized the material as an actuator, the other big application area enabled by ECO hydrogels, by measuring the pressure needed to compress a hydrogel to different degrees from its equilibrium swelling at applied potentials of −1 V, "off" and +1 V (**Figure 4**a). The shaded area between −1 V and "off" is the difference between the passive and ECO swelling pressure, showing the minimum electroactive operating range of actuation. This data allows us to separately measure the electroactive and the passive swelling pressures. The electroactive pressure at passive

equilibrium was 0.25 MPa (Figure S14a, Supporting Information), and the blocking pressure (the pressure needed to block ECO expansion completely) was 0.6–0.7 MPa (Figure 4a; Figure S14b, Supporting Information).[10] Applying +1 V before adding the electrolyte suppressed the passive swelling ("off"). Applying +1 V after passive swelling did not change the swelling pressure. However, after ECO expansion at −1 V, applying +1 V reduced the pressure measured under static conditions (Figure S15a, Supporting Information). Switching between +1 and −1 V with a cycle time of 10 min at 230% swelling vs dry changed the pressure by a factor 2 (Figure S15b, Supporting Information). From the shaded area in Figure 4a, the work density was calculated as ≈150 kJ m^{-3} or ≈120 J kg^{-1} (based on a density of 1.2 g cm^{-3} at 70 vol% water).

The pressure change induced by a positive potential is not sufficiently great to contract the network. However, one-way actuation is used in biological muscles, where the collagen–elastin lamina or counteracting muscles act as a restoring spring. Inspired by biological muscles, we applied a spring-back pressure opposite to the swelling direction (Figure 4b) using clamps (Figure S16, Supporting Information). With this spring-back mechanism, the hydrogel could be cycled with an ECO expansion of ≈25% at an initial rate of 17% min^{-1} at a pressure of 0.1 MPa, again demonstrating controllability that other hydrogel actuators lack. We further cycled an ECO actuator for 80 cycles without indication of loss of control and function (Figure S18, Supporting Information).

Table S1 (Supporting Information) compares state-of-the-art hydrogel actuators, and Figure 4c shows a quantitative
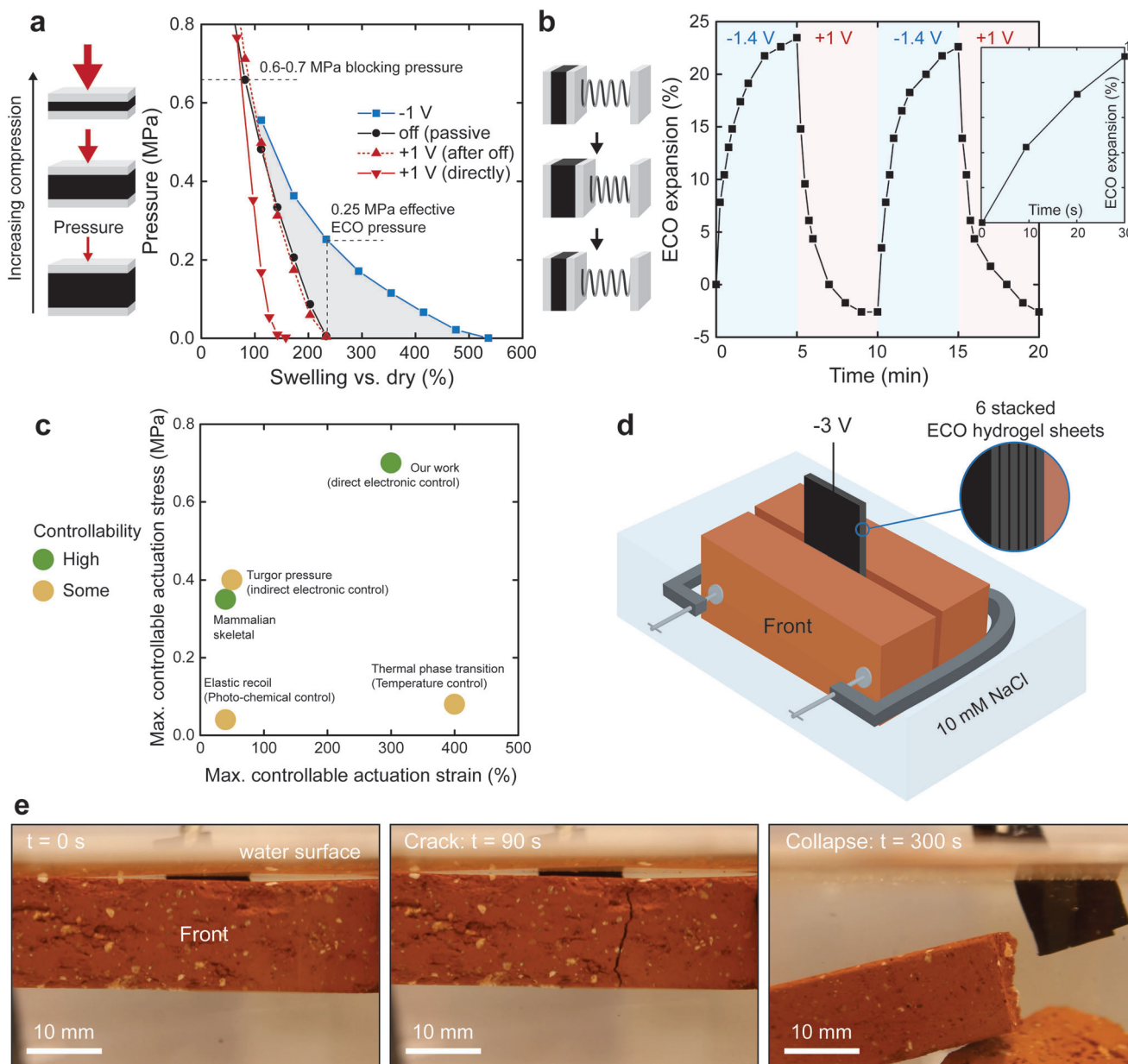
**ADVANCED
SCIENCE NEWS**

www.advancedsciencenews.com

**ADVANCED
MATERIALS**

www.advmat.de

Figure 4. Properties of the electrochemical osmotic actuation of ECO hydrogels. a) Property space of the actuation by normal force measurements. b) Schematic description of a spring-back mechanism and two reversible actuation cycles using a clamp as spring-back. The inset shows the initial 30 sec of the expansion. c) Comparison of hydrogel actuators (references in Table S1, Supporting Information). Green and orange, represent the degree of controllability (Table S1, Supporting Information) of the actuation. For controllable actuators, the strain is achieved by activation: total minus the passive that occurs just by placing the material in water. d) Illustration and the setup used to break a brick. Six sheets were stacked in this setup to achieve enough strain and work. The brick was 15 mm in height and 9 mm in thickness. e) Photographs of the process of breaking the brick (Video S1, Supporting Information) captured perpendicular to the plane of the ECO hydrogel. The conditions for the data in this figure are 45% CNTs and 10 mM NaCl. This demo pushed the limit of the actuator and the pressure needed was at least 0.5–0.7 MPa based on Figure 4a.

comparison of active and passive hydrogel actuators. Although there is inconsistency in reporting values, ECO actuators outperform most hydrogel actuators. They have a similar activated actuation strain as passive hydrogel actuators,[10] and at the same time higher actuation pressure and strain rate than turgor actuators.[13] This combination is enabled by the uniaxial expansion that directs the actuation pressure in one direction. The intrinsic electronic conductivity of ECO hydrogels allows high con-

trollability, which has been the main limitation of hydrogel actuators. The combination of high controllability with high pressure and high strain, the retained state, and permeability control are unique features of ECO hydrogels, paving the way for truly soft actuators and electrotunable membranes.

As a demonstration of its strength, we used the ECO actuator to break a brick 35 times thicker than the dry actuator (Figure 4d,e; Figure S17, Video S1, Supporting Information).

**ADVANCED
SCIENCE NEWS**

www.advancedsciencenews.com

**ADVANCED
MATERIALS**

www.advmat.de

This demonstrates its potential in high-strength applications and shows how ECO hydrogel sheets can easily be folded or stacked to tune their stroke.

3. Conclusion

We report electrochemically controlled nanowire composite hydrogels. The nanowire network makes them fundamentally different from other hydrogel actuators in at least four unique ways: i) They enable direct electronic control of their uniaxial expansion of up to 300% at a low voltage of −1 V. ii) Their expansion can be controlled in precise steps, as the network can be retained at any expanded state without consuming energy. iii) The self-sensed variable resistance can provide real-time feedback to control the expansion. iv) They exhibit inherent coupling between the expanded state and the mesoporosity of the hydrogel, enabling precise control of pore sizes for actively controlled separation, fractionation, or distribution of molecules, such as drugs or biomolecules, not easily achieved with dense polymeric membranes.

To describe the hydrogels, we derived an analytical model by adapting the Flory Rehner polyelectrolyte gel model to include the electrochemical properties of CNTs and the enthalpy elasticity of the network. Our work provides an initial coupled experimental and theoretical framework for fundamental studies linking electrochemistry and the colloidal chemistry of nanoparticle hydrogels.[35]

Two-way actuation (reversibility) without a spring-back is also a desirable feature, which we show is possible using the ECO principle in MXene-based nanocomposite hydrogels.[27]

To increase the actuation rate, we envision tuning the type of electrolyte and its concentration, reduce the cohesion in the network, or design of advanced structures with channels or holes to provide faster access to the electrolyte locally, which has been shown to improve the actuation rate of CNF sheets.[14]

Thanks to the abundance of CNFs and bulk electroactive nanomaterials, our multifunctional hydrogels can be easily produced in any lab and at scale. CNF nanocomposites can be shaped into advanced 3D objects, such as extruded threads or 3D-printed patterns,[36,37] taking us one step toward realizing soft intelligent systems where actuation, sensing, permeability control, and, in the future, ionotronic computation[3] are monolithically embedded.

Supporting Information

Supporting Information is available from the Wiley Online Library or from the author.

Conflict of Interest

The authors declare no conflict of interest.

Data Availability Statement

The data that support the findings of this study are available from the corresponding author upon reasonable request.

[1] M. A. Mcevoy, N. Correll, *Science* **2015**, *347*, 1261689.
[2] C. Yang, Z. Suo, *Nat. Rev. Mater.* **2018**, *3*, 125.
[3] A. Melianas, M.-A. Kang, A. Vahidmohammadi, T. J. Quill, W. Tian, Y. Gogotsi, A. Salleo, M. M. Hamedi, *Adv. Funct. Mater.* **2022**, *32*, 2109970.
[4] Y. Lee, W. J. Song, J.-Y. Sun, *Mater. Today Phys.* **2020**, *15*, 100258.
[5] Y. Lee, W. J. Song, Y. Jung, H. Yoo, M.-Y. Kim, H.-Y. Kim, J.-Y. Sun, *Sci. Rob.* **2020**, *5*, eaaz5405.
[6] S.-J. Jeon, A. W. Hauser, R. C. Hayward, *Acc. Chem. Res.* **2017**, *50*, 161.
[7] C.-Y. Lo, Y. Zhao, C. Kim, Y. Alsaid, R. Khodambashi, M. Peet, R. Fisher, H. Marvi, S. Berman, D. Aukes, X. He, *Mater. Today* **2021**, *50*, 35.
[8] P. Rothemund, Y. Kim, R. H. Heisser, X. Zhao, R. F. Shepherd, C. Keplinger, *Nat. Mater.* **2021**, *20*, 1582.
[9] Z. Zhang, J. Hao, *Adv. Colloid Interface Sci.* **2021**, *292*, 102408.
[10] W. R. K. Illeperuma, J.-Y. Sun, Z. Suo, J. J. Vlassak, *Soft Matter* **2013**, *9*, 8504.
[11] P. Techawanitchai, M. Ebara, N. Idota, T.-A. Asoh, A. Kikuchi, T. Aoyagi, *Soft Matter* **2012**, *8*, 2844.
[12] Y. S. Kim, M. Liu, Y. Ishida, Y. Ebina, M. Osada, T. Sasaki, T. Hikima, M. Takata, T. Aida, *Nat. Mater.* **2015**, *14*, 1002.
[13] H. Na, Y.-W. Kang, C. S. Park, S. Jung, H.-Y. Kim, J.-Y. Sun, *Science* **2022**, *376*, 301.
[14] T. Benselfelt, P. Rothemund, P. S. Lee, *Adv. Mater.* **2023**, *35*, 2300487.
[15] R. P. Hamlen, C. E. Kent, S. N. Shafer, *Nature* **1965**, *206*, 1149.
[16] H. B Schreyer, N. Gebhart, K. J. Kim, M. Shahinpoor, *Biomacromolecules* **2000**, *1*, 642.
[17] N. Mittal, F. Ansari, K. GowdaV, C. Brouzet, P. Chen, P. T. Larsson, S. V. Roth, F. Lundell, L. Wågberg, N. A. Kotov, L. D. Söderberg, *ACS Nano* **2018**, *12*, 6378.
[18] R. Östmans, M. F. Cortes Ruiz, J. Rostami, F. A. Sellman, L. Wågberg, S. B. Lindström, T. Benselfelt, *Soft Matter* **2023**, *19*, 2792.
[19] S. M. Mirvakili, I. W. Hunter, *Adv. Mater.* **2018**, *30*, 1704407.
[20] D. Morales, E. Palleau, M. D. Dickey, O. D. Velev, *Soft Matter* **2014**, *10*, 1337.
[21] T. Li, C. Chen, A. H. Brozena, J. Y. Zhu, L. Xu, C. Driemeier, J. Dai, O. J. Rojas, A. Isogai, L. Wågberg, L. Hu, *Nature* **2021**, *590*, 47.
[22] A. Hajian, S. B. Lindström, T. Pettersson, M. M. Hamedi, L. Wågberg, *Nano Lett.* **2017**, *17*, 1439.
[23] H. Koga, T. Saito, T. Kitaoka, M. Nogi, K. Suganuma, A. Isogai, *Biomacromolecules* **2013**, *14*, 1160.
[24] A. Hajian, Z. Wang, L. A. Berglund, M. M. Hamedi, *Adv. Electron. Mater.* **2019**, *5*, 1800924.

**ADVANCED
SCIENCE NEWS**

www.advancedsciencenews.com

**ADVANCED
MATERIALS**

www.advmat.de

[25] T. Benselfelt, L. Wågberg, *Biomacromolecules* **2019**, *20*, 2406.

[26] E. Prince, E. Kumacheva, *Nat. Rev. Mater.* **2019**, *4*, 99.

[27] L. Li, W. Tian, A. Vahid Mohammadi, J. Rostami, B. Chen, K. Matthews, F. Ram, T. Pettersson, L. Wågberg, T. Benselfelt, Y. Gogotsi, *Adv. Mater.* **2023**, https://doi.org/10.1002/adma.202301163.

[28] G. M. Spinks, G. G. Wallace, L. S. Fifield, L. R. Dalton, A. Mazzoldi, D. De Rossi, I. I. Khayrullin, R. H. Baughman, *Adv. Mater.* **2002**, *14*, 1728.

[29] T. Benselfelt, M. Nordenström, M. M. Hamedi, L. Wågberg, *Nanoscale* **2019**, *11*, 3514.

[30] T. Benselfelt, N. Kummer, M. Nordenstrom, A. B. Fall, G. Nystrom, L. Wagberg, *ChemSusChem* **2023**, *21*, 202201955.

[31] G. Li, X. Chen, F. Zhou, Y. Liang, Y. Xiao, X. Cao, Z. Zhang, M. Zhang, B. Wu, S. Yin, Y. Xu, H. Fan, Z. Chen, W. Song, W. Yang, B. Pan, J. Hou, W. Zou, S. He, X. Yang, G. Mao, Z. Jia, H. Zhou, T. Li, S. Qu, Z. Xu, Z. Huang, Y. Luo, T. Xie, J. Gu, et al., *Nature* **2021**, *591*, 66.

[32] H. Chu, X. Hu, Z. Wang, J. Mu, N. Li, X. Zhou, S. Fang, C. S. Haines, J. W. Park, S. Qin, N. Yuan, J. Xu, S. Tawfick, H. Kim, P. Conlin, M. Cho, K. Cho, J. Oh, S. Nielsen, K. A. Alberto, J. M. Razal, J. Foroughi, G. M. Spinks, S. J. Kim, J. Ding, J. Leng, R. H. Baughman, *Science* **2021**, *371*, 494.

[33] X. Tan, C. Hu, Z. Zhu, H. Liu, J. Qu, *Adv. Funct. Mater.* **2019**, *29*, 1903081.

[34] W.-S. Hung, S.-Y. Ho, Y.-H. Chiao, C.-C. Chan, W.-Y. Woon, M.-J. Yin, C.-Y. Chang, Y. M. Lee, Q.-F. An, *Chem. Mater.* **2020**, *32*, 5750.

[35] Y. Xue, Y. Xia, S. Yang, Y. Alsaid, K. Y. Fong, Y. Wang, X. Zhang, *Science* **2021**, *372*, 501.

[36] M. M. Hamedi, A. Hajian, A. B. Fall, K. Håkansson, M. Salajkova, F. Lundell, L. Wågberg, L. A. Berglund, *ACS Nano* **2014**, *8*, 2467.

[37] Y. Li, H. Zhu, Y. Wang, U. Ray, S. Zhu, J. Dai, C. Chen, K. Fu, S.-H. Jang, D. Henderson, T. Li, L. Hu, *Small Methods* **2017**, *1*, 1700222.

2303255 (9 of 9)